Effect of Nitrogen Doping and Acene Cores Elongation on Charge Transport and Electronic Nature of Organic Semiconductor Materials: A DFT Study

Irfan, Ahmad*[+•]

Department of Chemistry, Faculty of Science, King Khalid University, Abha 61413, P.O. Box 9004, SAUDI ARABIA

ABSTRACT: *With the intention to tune the charge transport nature of preliminary 4,6-di(thiophen-2-yl)pyrimidine (DTP) structure, six novel V-shaped organic semiconductor compounds were designed by nitrogen doping and acene moieties elongation. Initially, the nitrogen atoms were doped in DTP to design 4,6-bis-thiazol-2-yl-pyrimidine (**1**). Moreover, by □-bridge elongation strategy, 4,6-bis-benzo[b]thiazol-2-yl-pyrimidine (**2**), 4,6-bis(naphthothiazol-2-yl)pyrimidine (**3**), 4,6-bis(anthracenothiazol-2-yl)pyrimidine (**4**), 4,6-bis(tetracenothiazol-2-yl)pyrimidine (**5**), and 4,6-bis(pentacenothiazol-2-yl)pyrimidine (**6**) were designed by substituting various oligocenes at both ends. The ground, as well as excited state structures, were optimized using density functional theory (DFT) and time-dependent DFT at B3LYP/6-31G** and TD-B3LYP/6-31G** levels, correspondingly. We explored their frontier molecular orbitals, electron injection aptitude, photo-stability, Ionization Energies (IE), electron affinity (EA), and reorganization energies. The bridge elongation significantly elevates the EA while reducing the IE which would result in to decrease in the injection barrier for electron and hole transport. Furthermore, acene cores elongation expressively decreases the hole and electron reorganization energies as compared to frequently used materials pentacene and tris(8-hydroxyquinolinato)aluminum (mer-Alq3) which revealed that newly designed materials would be proficient to be used in p- and/or n-type semiconductor devices.*

KEYWORDS: *Organic semiconductors; Pentacene; tris(8-hydroxyquinolinato)aluminum; Charge transport; Electronic properties*

INTRODUCTION

The Organic Semiconductors Materials (OSMs) based on their carrier mobility have triggered research work to utilize compounds having applications for energy conversion, towards organic light-emitting diodes, optoelectronic along with photovoltaics [1-4]. Recently organic optoelectronics has evolved into numerous devices

***** *To whom correspondence should be addressed.*

+ *E-mail: irfaahmad@gmail.com*

● *Other Address: Research Center for Advanced Materials Science, King Khalid University, Abha 61413, P.O. Box 9004, SAUDI ARABIA*

1021-9986/2022/2/399-409 11/$/6.01

within Organic Light-Emitting Diodes (OLEDs), photovoltaics along with Organic Field-Effect Transistors (OFETs) [5-10]. Marcus' theory explained OSMs, electrons, or hole polarons cover the compounds with the hopping process. Aromatic compounds gained too much interest from synthetic as well as theoretical chemists [11] Based on their broad range of applications as organic semiconductors [12, 13]. The recent research on Polycyclic Conjugated Hydrocarbons (PCHs) has broadened its application in the organic electronics industry rapidly as well as to produce new functional compounds instead of inorganic solids [14-17]. The extended conjugation, stable as well as optoelectronic characteristics in PCHs (e.g., polyacenes) made them interesting OSMs. Based on inherent instability-many longer polyacenes dimerize and/or photooxidize easily within atmospheric surroundings except adequately stabilized [18]. Keeping in mind, the problems there is a need to synthesize polyacene substituents having better stability along with promising electronic characteristics.

To increase the charge carrier mobility values of OSMs analogous to amorphous silicon, either quantum proficiency of carrier generation because of light absorption is significant. These problems determination inhibited by their physical mechanisms and complications. To clarify the provided experimental records the computational analysis appeared extremely effective tool, through the calculation of novel materials characteristics along with unique functional systems designing. The steady demand for computational potential as well as advancement within complex software packages enabled computational investigations on a diversity of organic electronic substances along with systems that could be extremely hard to access in recent years [19].

Currently, computational analyses have been carried out to disclose the predicting strength with a first-principles approach towards the evaluation of Ionization Energy (IE) among conjugated compounds. Based on recent applications within photovoltaic devices the thiophene-based molecules IE calculation gained extraordinary attention. These modifications within the structure of these compounds are considered the best approach to adjust charge transport as well as the electro-optical properties of OSMs. The highest occupied molecular orbital (E_{HOMO}) energy, absorption (λ_{abs}) along with the energy of lowest unoccupied molecular orbital (E_{LUMO}), reorganization energy (λ), IE, and electron affinity (EA) were used to probe OSMs characteristics.

Density functional methods achieved high order maturation as well as attributed excellent predictive power for the calculation of molecular geometries along with formation energies. The extension of these approaches appears naturally over their original objective to address the non-equilibrium transport procedures with single (or few) compounds as well as to investigate their device operations. The DFT [20] computations for such a purpose generally enable the molecular system explanation with regard to electronic properties. The electronic interactions are equivalent to electron-phonon correlations in π-conjugated organic compounds that could be represented with λ which is inversely proportional to the rate of its charge transfer [21]. Intramolecular Charge Transfer (ICT) is used to enhance the rate of charge transfer, reducing the structural deviation along with polarization after electron-deficient groups incorporation [22]. These environmentally friendly, cost-effective, tiny organic compounds are usually easy to manufacture [23]. Furthermore, these tiny organic compounds after chain alignment accomplished wonderful charge transport and electro-optical characteristics. The enhanced electronic applications of these molecular structures after promising chain conformation [24, 25], are extremely fruitful with appropriate E_{HOMO}, E_{LUMO}, IE as well as EA [26]. For the fabrication of proficient OFETs, polyacenes were considered highly favorable compounds [27, 28]. For the management of the electrical properties of these tiny organic compounds, the π-conjugated cores, end groups and substitution of heteroatoms are favorable approaches [13]. Moreover, to enhance the charge transport characteristics, the introduction of various π-conjugated bridges within designed compounds would be a nice approach.

Previously, we have displayed that 4,6-di(thiophen-2-yl)pyrimidine (DTP) is an excellent building block to design efficient optoelectronic substances [22]. In order to further adjust charge transport as well as electro-optical characteristics, we designed different compounds. We have planned six new systems with some structural alteration through their ring size elongating as well as nitrogen doping. The obtained products include the following *i.e.*, the nitrogen atoms were doped in DTP to design 4,6-bis-thiazol-2-yl-pyrimidine (**1**). Moreover, by π-bridge elongation strategy, 4,6-bis-benzo[*b*]thiazol-2-yl-pyrimidine (**2**), 4,6-bis(naphthothiazol-2-yl)pyrimidine (**3**), 4,6-bis(anthracenothiazol-2-yl)pyrimidine (**4**), 4,6- bis(tetracenothiazol-2-yl)pyrimidine (**5**), and 4,6-

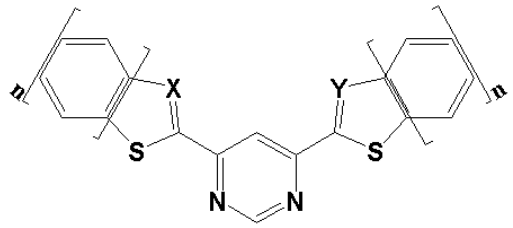

DTP; X, Y = C and n = 0 **1**; X, Y = N and n = 0
2; X, Y = N and n = 1 **3**; X, Y = N and n = 2
4; X, Y = N and n = 3 **5**; X, Y = N and n = 4
6; X, Y = N and n = 5

Fig. 1: The structures of DTP and derivatives examined in the current work.

bis(pentacenothiazol-2-yl)pyrimidine (**6**) were designed by substituting various Oligocene at both ends, as shown in Fig. 1.

A new methodology was prescribed comprehensively within the next section in detail. Furthermore, in the "RESALTS AND DISCUSSION" section the electronic properties, the distribution pattern of the frontier molecular orbitals and energies of HOMO and LUMO, and charge transport characteristics (vertical/adiabatic EA, vertical/adiabatic IE, and hole/electron λ) are discussed.

METHODOLOGY

The standard DFT functional (B3LYP) established the best explanation regarding geometry alterations upon ionization [29] in ground state (S_0) optimization. Currently, 6-31G** basis set [30] level using B3LYP [31] functional were used for theoretical computations. The TDDFT has been used for the λ_{abs} calculation proving it as an efficient methodology [32]. The charge transport capability performs a central function within the various organic layer(s). The recombination processes in the bulk are supported by their higher-charge mobility in which charges could be limited through organic–organic interfaces [33]. Marcus' theory is used for the measurement of the rate of charge transfer as per equation 1 [34].

$$W = V^2 / h\left(\pi / \lambda k_B T\right)^{1/2} \exp\left(-\lambda / 4 k_B T\right) \quad (1)$$

The rates of self-exchange electron-transfer along with their charge mobility used to calculate with two major standards: (i) λ, which should be small for significant transport, along with (ii) neighboring compounds transfer integral (V) or electronic coupling which should be optimized. The term λ characterizes the intensity regarding electron-phonon interactions (vibration) and it was evaluated doubled compared with polaron localized relaxation energy considering individual entity. The λ unit may be segregated into two components: $\lambda_{rel}^{(1)}$ and $\lambda_{rel}^{(2)}$. The relaxation energy geometry for one compound from neutral to charged state resembles $\lambda_{rel}^{(1)}$ and relaxation energy geometry from the same compound from charged to neutral state corresponds to $\lambda_{rel}^{(2)}$ [35].

$$\lambda = \lambda_{rel}^{(1)} + \lambda_{rel}^{(2)} \quad (2)$$

For λ, the two other terms were calculated with the help of adiabatic potential energy surfaces directly. The assessment of the two-component of λ was determined quickly in accordance with adiabatic potential energy surfaces with the help of Eq. (2) [36].

$$\lambda = \lambda_{rel}^{(1)} + \lambda_{rel}^{(2)} = \left[E^{(1)}\left(L^+\right) - E^{(0)}\left(L^+\right)\right] + \left[E^{(1)}(L) - E^{(0)}(L)\right] \quad (3)$$

In above Eq. (2,) the terms $E^{(0)}(L)$, $E^{(0)}(L^+)$ represents neutral ground-state energies (optimized) along with charged ones. The $E^{(1)}(L)$ is neutral compound energy with optimized charged geometry whereas $E^{(1)}(L^+)$ is the energy of the charged state with the geometry of the optimized neutral compound. It is important to observe that surrounding compounds' polarization impact along with the realignment of their charges were ignored in order to reduce the theoretical computational complications [37]. By using the theory of B3LYP/6-31G** level, the values of EAa/v and IEa/v were calculated. All computations analyses were performed with the help of Gaussian16 software [38].

RESULTS AND DISCUSSION

Electronic properties

The computed values of energies of the frontier molecular orbitals, *i.e.*, HOMO/LUMO energies (E_{HOMO}/E_{LUMO}) and their energy gaps (E_{gap}) displayed in Table 1. The estimated values of E_{HOMO}/E_{LUMO} of DTP were -6.19/-1.94 at ground state (S_0), respectively [39]. The computed E_{HOMO}/E_{LUMO} of designed derivatives are -6.60/-2.35, -6.46/-2.51, -5.73/-2.64, -5.24/-2.83, -4.91/-2.73 and -4.66/-2.92 at S_0, respectively. It can be observed that nitrogen doping lowers the E_{HOMO} and E_{LUMO} levels. Additionally, π-bridge elongation higher the E_{HOMO} while

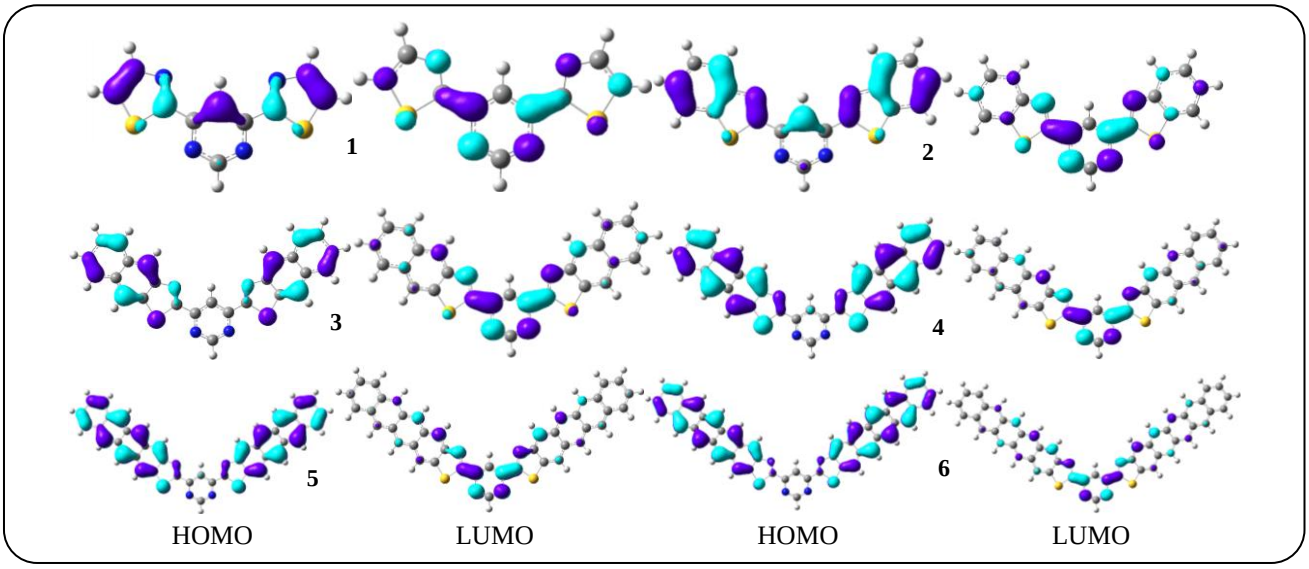

Fig. 2: Distribution pattern of the frontier molecular orbitals of studied compounds at ground states.

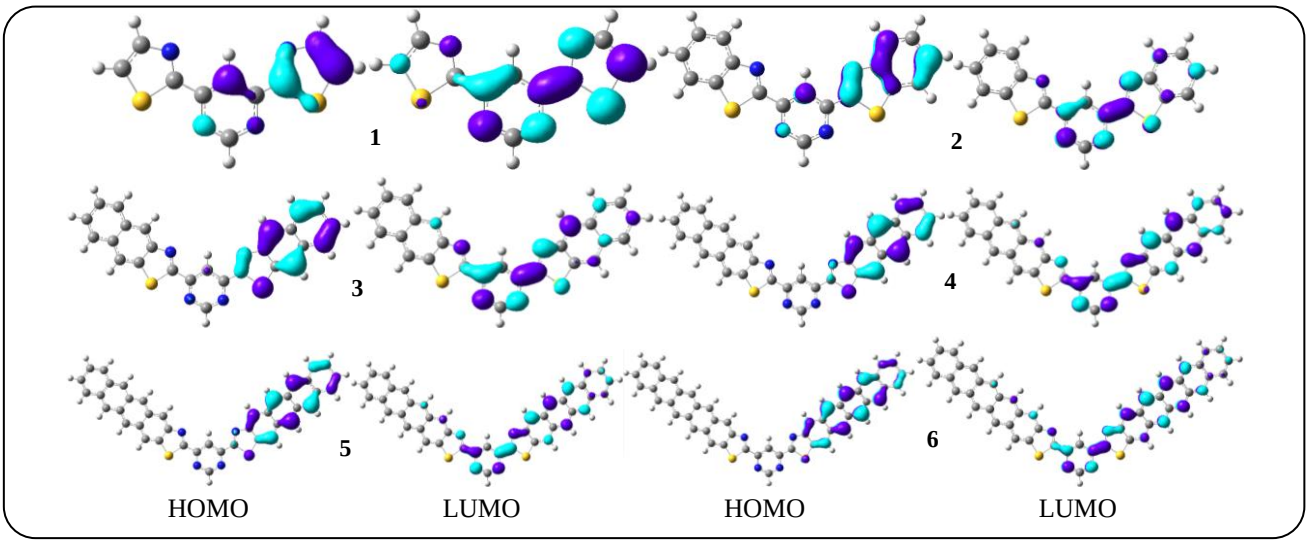

Fig. 3: Distribution pattern of the HOMOs and LUMOs at excited states.

lower the E_{LUMO} levels resulting in reducing the E_{gap}. This strategy of integration would be helpful for designing *p*- as well as *n*-type efficient materials. The trend in the E_{gaps} was found as DTP (4.25) = **1** (4.25) > **2** (3.95) > **3** (3.09) > **4** (2.51) > **5** (2.08) > **6** (1.74) eV. The E_{gap} is significantly decreased after the incorporation of pentacene moieties at both ends from 4.25 to 1.74 eV. The estimated values of E_{HOMO}/E_{LUMO} of DTP were -6.02/-2.10 at the excited state (S_1), respectively [39]. The computed E_{HOMO}/E_{LUMO} of designed derivatives are -6.23/-2.68, -6.14/-2.83, -5.55/-2.86, -4.86/-2.90, -4.67/-2.94, and -4.51/-3.00 at S_1, respectively. It can be observed that nitrogen doping lowers the E_{HOMO} and E_{LUMO} levels. Additionally, π-bridge elongation higher the E_{HOMO} while lower the E_{LUMO} levels as compared to **1** resulting to reduce E_{gap}. The trend in the E_{gaps} was found as DTP (3.92) > **1** (3.55) > **2** (3.31) > **3** (2.69) > **4** (1.96) > **5** (1.73) >**6** (1.51) eV.

The E_{gap} is significantly decreased after the incorporation of pentacene moieties at both ends from 3.55 to 1.51 eV. It is anticipated that this approach of assimilation would help design longer wavelengths and efficient semiconductor materials.

HOMOs and LUMOs formation patterns for studied compounds along with its derived compounds at S_0 and S_1

Table 1: The ground and first excited states HOMO/LUMO energies (E_{HOMO}/E_{LUMO}), and their gaps (E_{gap}) in eV calculated at B3LYP/6-31G** and TD-B3LYP/6-31G** levels, respectively.

Complexes	Ground state			First excited state		
	E_{HOMO}	E_{LUMO}	E_{gap}	E_{HOMO}	E_{LUMO}	E_{gap}
DTP	-6.19	-1.94	4.25	-6.02	-2.10	3.92
1	-6.60	-2.35	4.25	-6.23	-2.68	3.55
2	-6.46	-2.51	3.95	-6.14	-2.83	3.31
3	-5.73	-2.64	3.09	-5.55	-2.86	2.69
4	-5.24	-2.73	2.51	-4.86	-2.90	1.96
5	-4.91	-2.83	2.08	-4.67	-2.94	1.73
6	-4.66	-2.92	1.74	-4.51	-3.00	1.51

Table 2: The electron injection energy (EIE) and hole injection energy (HIE) (in eV) of DTP derivatives calculated at B3LYP/6-31G** level.

Parameters	DTP	1	2	3	4	5	6
HIE (Au)	1.09	1.50	1.36	0.63	0.14	-0.19	-0.44
EIE (Au)	3.16	2.75	2.59	2.46	2.37	2.27	2.18
HIE (Al)	2.11	2.52	2.38	1.65	1.16	0.83	0.58
EIE (Al)	2.14	1.73	1.57	1.44	1.35	1.25	1.16

were presented within Figs. 2 and 3. At S_0, in the formation of HOMO charge has been delocalized on sides while LUMO localized on the central electron-deficient ring. In all studied molecules the Intra-molecular Charge Transport (ICT) was perceived from occupied to unoccupied molecular orbitals. At S_1, HOMO charge density is delocalized on the right moiety while LUMO is localized at the central pyrimidine core.

The work functions (W) with regards Au and Al electrodes are 5.10 and 4.08 eV, respectively [40]. From this, we inspected hole/electron injection energies (HIE/EIE) of DTP and derivatives (**1-6**) with respect to Au and Al electrodes individually as (EIE = $-E_{LUMO}$ − (−W of metal)) and (HIE = − W of metal − ($-E_{HOMO}$). The results of theoretical EIE revealed that **1-6** could show more assistance for hole and electron injection when compared with DTP. Furthermore, it can be observed that Al/Au may be an appropriate electrode for its better ability towards electron and hole injection for **1-4**, respectively see Table 2. When Al/Au electrode was used the EIE/HIE energy hurdle are significantly lessened after Oligocene groups incorporation. From the results, it is predicted that this method would be supportive of designing improved hole and electron injection materials for semiconductor substances.

The essential parameters like Global Chemical Reactivity Descriptors (GCRD) are used to figure out the reactivity and structural stability. Currently, we have computed GCRD theoretical parameters as for example softness (S), electronegativity (χ), chemical potential (μ), chemical hardness (η) along with electrophilicity index (ω) values for DTP-derived products with the help of IE and EA, see Table 3.

An approximation for absolute hardness η was developed as given below[41-43]:

$$\eta = \frac{IE - EA}{2} \quad (4)$$

Where *IE* is the vertical ionization energy and *EA* is the vertical electron affinity.

Values of *IE* and *EA* calculated are given in Table 4. The lower energy of IE corresponds to the more reactive molecule in the reactions with electrophiles, while lower EA energy is essential for molecular reactions with nucleophiles [44].

Table 3: The η, μ, S, χ, and ω in eV of DTP and derivatives at B3LYP/6-31G** level.

Parameters	DTP	1	2	3	4	5	6
Hardness (η)	3.62	3.65	3.27	2.69	2.26	1.94	1.69
Potential (μ)	-4.06	-4.46	-4.44	-3.13	-3.94	-3.83	-3.77
Softness (S)	1.05	1.11	1.18	1.27	1.37	1.48	1.61
Electronegativity (χ)	4.06	3.46	4.44	4.13	3.94	3.83	3.77
Electrophilic index (ω)	2.27	2.73	3.02	3.17	3.43	3.78	4.20

Hence, the hardness of any material is corresponds to the gap between the IE and EA orbitals. If the energy gap of HOMO-LUMO is larger then the molecule would be harder [42].

$$\eta = \frac{1}{2}(EA - IE) \quad (5)$$

The electronic chemical potential (μ) of a molecule is calculated by:

$$\mu = \left(\frac{IE + EA}{2}\right) \quad (6)$$

The softness of a molecule is calculated by:

$$S = \frac{1}{2\eta} \quad (7)$$

The electronegativity of the molecule is calculated by:

$$\chi = \left(\frac{IE + EA}{2}\right) \quad (8)$$

The electrophilicity index of the molecule is calculated by:

$$\omega = \frac{\mu^2}{2\eta} \quad (9)$$

The calculated values of GCRD such as *η, μ, S, χ,* and *ω* for studied molecules are also presented in Table 3.

The *η* of the molecule is interrelated to aromaticity [45, 46]. The *μ* expresses the electron tendency to get await from its electronic cloud environment. The η value represents the degree of impediment of the electronic cloud distortion and stabilization energy values denote ω. The obtained values of μ demonstrated the incorporation of acene groups within the parent molecule, the tendency to provide particles in newly designed derivatives (**2-6**) might be smaller than DTP which can additionally increase the stability.

Molecular Electrostatic Potential (MEP)

The MEP is an appropriate parameter to examine the reactivity of different molecules and/or species. Actually, MEP is a noticeable property that could be experimentally evaluated through a diffraction spectrum [47, 48]. Furthermore, it might be explored through computational resources. It also demonstrates the broad range of nuclear and electronic charge allocation that is an applicable aspect to figure out different species interactions. The color displays in Fig. 4 showed designed derivatives MEP mapped. Within MEP, the higher negative potential zones indicated through the red color spot are helpful in order for electrophilic substitution, while higher positive potential zones showed with the blue color spot classify favorable towards nucleophilic substitution attack. The positive MEP reduces according to the following color ordering blue > green > yellow > orange > red. The greater repulsion was observed in red color areas whereas the blue color area explained the adequate attraction for nucleophilic attack and vice versa.

The negative electrostatic potential was found on the -N atoms while the positive one was on hydrogen atoms. It is anticipated that substantial repulsion would be at –N atoms along with significant attraction toward hydrogen atoms wherein nucleophilic attack occurs. Whereas for instance, electrophilic substitution occurs, significant repulsion could occur towards -H atoms along with notable attraction would be at –N atoms, see Fig. 4. As a hole, by elongating the side chains, e.g. **2-6** are showing more negative electrostatic potential on entire systems in the order **6** > **5** > **4** > **3** > **2** > **1**. Previously, the photostability of organic compounds was discussed by considering the MEP, *i.e.* more electron potential might enhance the photostability [49]. It was shown that the negative potential of the compound might hinder the photooxidation resulting to favor in improving the photostability [49]. It can be found in newly designed derivatives that by the chain

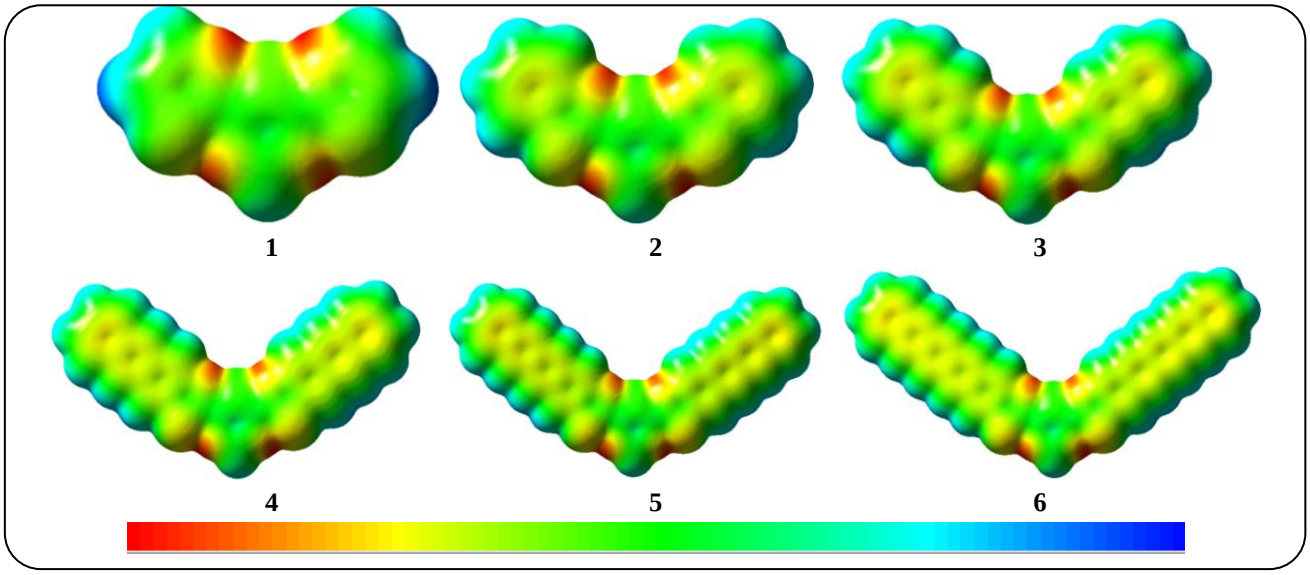

Fig. 4. MEP of studied compounds.

elongation negative potential also increased at both sides of the DTP which might make oxidation more difficult and improve the photostability.

Charge transport properties

The EA and IE are remarkable characteristics that would provide assistance to comprehend the charge transport barrier. The IE and EA values were obtained with B3LYP/6-31G** level computation studies and are exhibited in Table 4. Among organic semiconducting substances, the higher EA will give rise to greater electron transport performance while lower IE is very important to boost up the whole charge transport competency. The computed adiabatic/vertical IE (IEa/IEv) and adiabatic/vertical EA (EAa/EAv) of studied compounds (**1-6**) were presented in Table 4.

The results showed that nitrogen doping in DTP increased the $IE_{a/v}$, *i.e.*, 420/440 meV while $EA_{a/v}$, *i.e.*, 410/380 meV for **1** as compared with DTP, respectively. Furthermore, it can be observed that elongating the acene cores at both ends lowers $IE_{a/v}$ values as 370/400, 1220/1300, 1820/1910, 2250/2340, and 2560/2620 meV for **2-6** as compared to compound **1**, respectively. It can be perceived that elongating the acene cores at both ends considerably enhances the $EA_{a/v}$, *i.e.*, 360/360, 630/630, 830/870, 1020/1080, and 1190/1270 eV for **2-6** than that of compound **1**, correspondingly. The $IE_{a/v}$ and $EA_{a/v}$ of **2-6** are smaller and greater than **1**, respectively resulting in lessening the charge injection barrier. The obtained results revealed that designed derivatives (**2-6**) might have better hole along with electron charge injection capability compared with **1**. The lower/higher IE/EA disclosed the fact that these designed derivatives might be good *p*- and *n*-type materials.

The extremely important parameter λ is the quantity that is used for the assessment of the substance's ability to carry out a charge [36, 50]. The estimated λ value at B3LYP/6-31G** level for electron λ(e)/hole λ(h) is displayed in Table 4. It can be seen that nitrogen doping in DTP increases the λ(h) and λ(e), *i.e.*, 37 and 65 meV, respectively. One can see that acene fusion at both ends helps to decrease the λ(h) in designed compounds **2-6**, *i.e.*, 52, 165, 177, 181, and 186 meV than that of **1**. On other hand, acene fusion at both ends also helps to decrease the λ(e) in designed compounds **3-6**, *i.e.*, 29, 87, 143, and 182 meV than that of **1**. The λ(h), as well as λ(e), were associated with well-known referenced compounds giving an explanation of the charge transport behavior of newly designed products. The computed λ(h) is smaller as compared to λ(e) within studied systems disclosing that these compounds may act as best hole transport candidates. The λ(h) of **3-6** are smaller than the anthra[2,3-b:7,8-b^0] dithiophene (λ(h), 0.096) and anthra[2,3-b:8,7-b^0] dithiophene (λ(h), 0.085) reference molecules [39] *i.e.*, 22, 34, 38 and 43 meV as well as 11, 23, 27 and 32 meV, respectively. The calculated results showed that pentacene is a proficient hole transport substance. *Gruhn et al.* exhibited that λ is the crucial constituent that allows

Table 4: The ionization energies, electronic affinities, reorganization energies (λ (h), and λ (e)) (in eV) at the B3LYP/6-31G** level.

Complexes	IEa	EAa	IEv	EAv	λ (h)	λ (e)
DTP	7.58	0.54	7.68	0.43	0.202	0.228
1	8.00	0.95	8.12	0.81	0.239	0.293
2	7.63	1.31	7.72	1.17	0.187	0.295
3	6.78	1.58	6.82	1.44	0.074	0.264
4	6.18	1.78	6.21	1.68	0.062	0.206
5	5.75	1.97	5.78	1.89	0.058	0.150
6	5.44	2.14	5.46	2.08	0.053	0.111

pentacene to vindicate the particularly higher hole mobility [51]. The value of λ(h) of pentacene was computed 0.098 eV [52]. The value of λ(h) of anthracene, naphthalene, along with tetracene at B3LYP/6-31G** levels are 0.138, 0.186, and 0.114, respectively [53]. The results of Table 4, showed that the λ(h) of newly designed products **3-6** are 24, 36, 40, and 45 meV smaller than the pentacene, respectively enlightening that these newly designed molecules could be excellent/comparable hole transport substance as of pentacene. For the newly designed molecules (**3-6**), λ(h) is lower compared to anthracene, naphthalene, tetracene as well as pentacene which demonstrated that these compounds might act as excellent hole transfer substances. Furthermore, the computational λ(e) of prominent used electron transport material *mer*-Alq3, value is 0.276 eV [54]. The results showed that values for λ(e) of **3-6** are 10, 70, 126, and 165 meV lower than the *mer*-Alq3 demonstrating that for these derivatives electron mobility values may be enhanced/comparable with *mer*-Alq3. Thus, it is anticipated that **3-6** would be efficient materials to be used as *p*- and *n*-type in semiconductor devices.

CONCLUSIONS

The HOMO-LUMO energy gaps significantly decreased after pentacene incorporation at both ends of the parent compound revealed this approach of assimilation would be helpful for designing materials with longer wavelengths for semiconductors. The intra-molecular charge transfer was observed from occupied to unoccupied molecular orbitals at the ground as well as excited states. The smaller the hole and electron injection barriers, the smaller ionization energy and larger electron affinity values of newly designed derivatives (**3-6**) revealing that these compounds would have good charge transfer ability which can ultimately enhance the intrinsic hole/electron mobility of semiconductors. The inclusion of acene groups at both ends of the parent compound significantly decreases the hole and electron reorganization energy values. The newly designed compounds (**3-6**) have smaller hole reorganization values compared with the commonly used reference molecules anthra [2,3-b:7,8-b^0] dithiophene, anthra [2,3-b:8,7-b^0] dithiophene, anthracene, naphthalene, tetracene as well as pentacene. The results enlightening that our designed compounds should act as excellent hole transfer materials that may be best/comparable to frequently used *p*-type ones. These designed compounds (**3-6**) also show smaller electron reorganization energy values which exhibited that these may be best/comparable with normally used *n*-type *mer*-Alq3. These results are revealing that the newly designed compounds (**3-6**) would have a good hole and electron intrinsic mobility and thus can be used in semiconductor devices.

Acknowledgments

I would like to acknowledge the financial support from Deanship of Scientific Research at the King Khalid University, Kingdom of Saudi Arabia for funding through the research groups program under grant number R.G.P.2/91/41.

Received : Aug. 3, 2020 ; Accepted : Nov. 2, 2020

REFERENCES

[1] Zhou R., Yang C., Zou W., Abdullah Adil M., Li H., Lv M., Huang Z., Lv M., Zhang J., Lu K., Wei Z., Combining Chlorination and Sulfuration Strategies for High-Performance All-Small-Molecule Organic Solar Cells, *J Energy Chem.*, **52**: 228-233 (2021).

[2] Seif N., Farhadi A., Badri R., Kiasat A.R., An Experimental and Theoretical Study on Bicyclo-3,4-Dihydropyrimidinone Derivative: Synthesis and DFT Calculation, *Iran. J. Chem. Chem. Eng. (IJCCE)*, **39(5)**: 21-33 (2019).

[3] Khalil Warad I., Al-Nuri M., Ali O., Abu-Reidah I.M., Barakat A., Ben Hadda T., Zarrouk A., Radi S., Touzani R., Hicham E., Synthesis, Physico-Chemical, Hirschfield Surface and DFT/B3LYP Calculation of Two New Hexahydropyrimidine Heterocyclic Compounds, *Iran. J. Chem. Chem. Eng. (IJCCE)*, **38(4)**: 59-68 (2019).

[4] Demirtaş G., Dege N., Ağar E., Şahin S., The Crystallographic, Spectroscopic and Theoretical Studies on (E)-2-[((4-Fluorophenyl)Imino)Methyl]-4-Nitrophenol and (E)-2-[((3-Fluorophenyl)Imino) Methyl]-4-Nitrophenol Compounds, *Iran. J. Chem. Chem. Eng. (IJCCE)*, **37(5)**: 55-65 (2018).

[5] Mesta M., Carvelli M., de Vries R.J., van Eersel H., van der Holst J.J.M., Schober M., Furno M., Lüssem B., Leo K., Loebl P., Coehoorn R., Bobbert P.A., Molecular-Scale Simulation of Electroluminescence in a Multilayer White Organic Light-Emitting Diode, *Nature Materials*, **12(7)**: 652-658 (2013).

[6] Green M.A., Emery K., Hishikawa Y., Warta W., Dunlop E.D., Solar Cell Efficiency Tables (Version 39), *Prog. Photovolt.*, **20(1)**: 12-20 (2012).

[7] Shrestha S., Photovoltaics Literature Survey (No. 104), *Prog. Photovolt.*, **21(6)**: 1429-1431 (2013).

[8] Irfan A., Al-Sehemi A.G., Assiri M.A., Mumtaz M.W., Exploring the Electronic, Optical and Charge Transfer Properties of Acene-Based Organic Semiconductor Materials, *Bull. Mat. Sci.*, **42(4)**: 145 (2019).

[9] Irfan A., Imran M., Thomas R., Mumtaz M.W., Qayyum M.A., Ullah S., Assiri M.A., Al-Sehemi A.G., Exploration of Electronic Nature and Intrinsic Mobility of 10-(1,3-Dithiol-2-Ylidene)Anthracene Based Organic Semiconductor Materials, *Optik*: 165530 (2020).

[10] Irfan A., Rasool Chaudhry A., Al-Sehemi A.G., Electron Donating Effect of Amine Groups on Charge Transfer and Photophysical Properties of 1,3-Diphenyl-1h-Pyrazolo[3,4-b]Quinolone at Molecular and Solid State Bulk Levels, *Optik*, **208**: 164009 (2020).

[11] Krygowski T.M., Cyrañski M.K., Czarnocki Z., Häfelinger G., Katritzky A.R., Aromaticity: A Theoretical Concept of Immense Practical Importance, *Tetrahedron*, **56(13)**: 1783-1796 (2000).

[12] Cao J., London G., Dumele O., von Wantoch Rekowski M., Trapp N., Ruhlmann L., Boudon C., Stanger A., Diederich F., The Impact of Antiaromatic Subunits in [4n+2] Π-Systems: Bispentalenes with [4n+2] Π-Electron Perimeters and Antiaromatic Character, *J. Am. Chem. Soc.*, **137(22)**: 7178-7188 (2015).

[13] Mei J., Diao Y., Appleton A.L., Fang L., Bao Z., Integrated Materials Design of Organic Semiconductors for Field-Effect Transistors, *J. Am. Chem. Soc.*, **135(18)**: 6724-6746 (2013).

[14] Bendikov M., Wudl F., Perepichka D.F., Tetrathiafulvalenes, Oligoacenenes, and Their Buckminsterfullerene Derivatives: The Brick and Mortar of Organic Electronics, *Chem. Rev.*, **104(11)**: 4891-4946 (2004).

[15] Anthony J.E., Facchetti A., Heeney M., Marder S.R., Zhan X., *n*-Type Organic Semiconductors in Organic Electronics, *Adv. Mater.*, **22(34)**: 3876-3892 (2010).

[16] Eftaiha A.a.F., Sun J.-P., Hill I.G., Welch G.C., Recent Advances of Non-Fullerene, Small Molecular Acceptors for Solution Processed Bulk Heterojunction Solar Cells, *J. Mater. Chem. A*, **2(5)**: 1201-1213 (2014).

[17] Wang Y., Fang D., Fu T., Ali M.U., Shi Y., He Y., Hu Z., Yan C., Mei Z., Meng H., Anthracene Derivative Based Multifunctional Liquid Crystal Materials for Optoelectronic Devices, *Mater. Chem. Front.* (2020).

[18] Zade S.S., Zamoshchik N., Reddy A.R., Fridman-Marueli G., Sheberla D., Bendikov M., Products and Mechanism of Acene Dimerization. A Computational Study, *J. Am. Chem. Soc.*, **133(28)**: 10803-10816 (2011).

[19] Baroudi B., Argoub K., Hadji D., Benkouider A.M., Toubal K., Yahiaoui A., Djafri A., Synthesis and DFT Calculations of Linear and Nonlinear Optical Responses of Novel 2-Thioxo-3-N,(4-Methylphenyl) Thiazolidine-4 One, *J. Sulfur Chem.*, **41(3)**: 310-325 (2020).

[20] Di Ventra M., Pantelides S.T., Lang N.D., First-Principles Calculation of Transport Properties of a Molecular Device, *Phys. Rev. Lett.*, **84(5)**: 979-982 (2000).

[21] Ran X.-Q., Feng J.-K., Ren A.-M., Li W.-C., Zou L.-Y., Sun C.-C., Theoretical Study on Photophysical Properties of Ambipolar Spirobifluorene Derivatives as Efficient Blue-Light-Emitting Materials, *J. Phys. Chem. A*, **113(27)**: 7933-7939 (2009).

[22] Irfan A., Muhammad S., Chaudhry A.R., Al-Sehemi A.G., Jin R., Tuning of Optoelectronic and Charge Transport Properties in Star Shaped Anthracenothiophene-Pyrimidine Derivatives as Multifunctional Materials, *Optik*, **149**(Supplement C): 321-331 (2017).

[23] Zhang J., Wu G., He C., Deng D., Li Y., Triphenylamine-Containing D-A-D Molecules with (Dicyanomethylene)Pyran as an Acceptor Unit for Bulk-Heterojunction Organic Solar Cells, *J. Mater. Chem.*, **21(11)**: 3768-3774 (2011).

[24] Minemawari H., Yamada T., Matsui H., Tsutsumi J.y., Haas S., Chiba R., Kumai R., Hasegawa T., Inkjet Printing of Single-Crystal Films, *Nature*, **475**: 364-367 (2011).

[25] Kim D.H., Park Y.D., Jang Y., Yang H., Kim Y.H., Han J.I., Moon D.G., Park S., Chang T., Chang C., Joo M., Ryu C.Y., Cho K., Enhancement of Field-Effect Mobility Due to Surface-Mediated Molecular Ordering in Regioregular Polythiophene Thin Film Transistors, *Adv. Funct. Mater.*, **15(1)**: 77-82 (2005).

[26] Wang L., Nan G., Yang X., Peng Q., Li Q., Shuai Z., Computational Methods for Design of Organic Materials with High Charge Mobility, *Chem. Soc. Rev.*, **39(2)**: 423-434 (2010).

[27] Anthony J.E., The Larger Acenes: Versatile Organic Semiconductors, *Angew. Chem. Int. Ed.*, **47(3)**: 452-483 (2008).

[28] Anthony J.E., Functionalized Acenes and Heteroacenes for Organic Electronics, *Chem. Rev.*, **106(12)**: 5028-5048 (2006).

[29] Sánchez-Carrera R.S., Coropceanu V., da Silva Filho D.A., Friedlein R., Osikowicz W., Murdey R., Suess C., Salaneck W.R., Brédas J.-L., Vibronic Coupling in the Ground and Excited States of Oligoacene Cations, *J. Phys. Chem. B*, **110(38)**: 18904-18911 (2006).

[30] Petersson G.A., Bennett A., Tensfeldt T.G., Al-Laham M.A., Shirley W.A., Mantzaris J., A Complete Basis Set Model Chemistry. I. The Total Energies of Closed-Shell Atoms and Hydrides of the First-Row Elements, *J. Chem. Phys.*, **89(4)**: 2193-2218 (1988).

[31] Lee C., Yang W., Parr R.G., Development of the Colle-Salvetti Correlation-Energy Formula into a Functional of the Electron Density, *Phys. Rev. B*, **37(2)**: 785-789 (1988).

[32] Zhang C., Liang W., Chen H., Chen Y., Wei Z., Wu Y., Theoretical Studies on the Geometrical and Electronic Structures of N-Methyle-3,4-Fulleropyrrolidine, *J. Mol. Struct. (TheoChem)*, **862(1–3)**: 98-104 (2008).

[33] Greenham N.C., Moratti S.C., Bradley D.D.C., Friend R.H., Holmes A.B., Efficient Light-Emitting Diodes Based on Polymers with High Electron Affinities, *Nature*, **365(6447)**: 628-630 (1993).

[34] Marcus R.A., Sutin N., Electron Transfers in Chemistry and Biology, *Biochim. Biophys. Acta - Rev. Bioenerg.*, **811(3)**: 265-322 (1985).

[35] Tsiper E.V., Soos Z.G., Gao W., Kahn A., Electronic Polarization at Surfaces and Thin Films of Organic Molecular Crystals: PTCDA, *Chem. Phys. Lett.*, **360(1–2)**: 47-52 (2002).

[36] Brédas J.L., Calbert J.P., da Silva Filho D.A., Cornil J., Organic Semiconductors: A Theoretical Characterization of the Basic Parameters Governing Charge Transport, *Proc. Natl. Acad. Sci.*, **99(9)**: 5804-5809 (2002).

[37] Soos Z.G., Tsiper E.V., Painelli A., Polarization in Organic Molecular Crystals and Charge-Transfer Salts, *J. Lumin.*, **110(4)**: 332-341 (2004).

[38] Frisch M.J., Trucks G.W., Schlegel H.B. et al., Gaussian-16, Revision A.1, Gaussian, Inc., Wallingford, CT. 2016.

[39] Irfan A., Rasool Chaudhry A., G. Al-Sehemi A., Sultan Al-Asiri M., Muhammad S., Kalam A., Investigating the Effect of Acene-Fusion and Trifluoroacetyl Substitution on the Electronic and Charge Transport Properties by Density Functional Theory, *J. Saudi. Chem. Soc.*, **20(3)**: 336-342 (2016).

[40] Irfan A., Imran M., Thomas R., Basra M.A.R., Ullah S., Al-Sehemi A.G., Assiri M.A., Exploring The Effect of Oligothiophene and Acene Cores nn the Optoelectronic Properties and Enhancing p- and n-Type Ability of Semiconductor Materials, *J. Sulfur Chem.*, (2020).

[41] Pearson R.G., The Principle of Maximum Hardness, *Acc. Chem. Res.*, **26**: 250-255 (1993).

[42] Pearson R.G., Absolute Electronegativity and Absolute Hardness of Lewis Acids and Bases, *J. Am. Chem. Soc.*, **107(24)**: 6801-6806 (1985).
[43] Parr R.G., Pearson R.G., Absolute Hardness: Companion Parameter to Absolute Electronegativity, *J. Am. Chem. Soc.*, **105(26)**: 7512-7516 (1983).
[44] Rauk A., Orbital Interaction Theory of Organic Chemistry, 2nd ed., John Wiley & Sons, Inc.: Newyork, **34**: (2001).
[45] Vektariene A., Vektaris G., Svoboda J., A Theoretical Approach to the Nucleophilic Behavior of Benzofused Thieno[3,2-B]Furans Using DFT and HF Based Reactivity Descriptors, *ARKIVOC*, **2009(7)**: 311-329 (2009).
[46] Geerlings P., De Proft F., Langenaeker W., Conceptual Density Functional Theory, *Chem. Rev.*, **103(5)**: 1793-1874 (2003).
[47] Politzer P., Truhlar (Eds.) D.G., "Chemical Applications of Atomic and Molecular Electrostatic Potentials", Springer, Boston, MA, (1981).
[48] Stewart R.F., On the Mapping of Electrostatic Properties from Bragg Diffraction Data, *Chem. Phys. Lett.*, **65(2)**: 335-342 (1979).
[49] Irfan A., Zhang J., Chang Y., Theoretical Investigations of the Charge Transfer Properties of Anthracene Derivatives, *Theor. Chem. Acc.*, **127(5)**: 587-594 (2010).
[50] Marcus R.A., Electron Transfer Reactions in Chemistry. Theory and Experiment, *Rev. Mod. Phys.*, **65(3)**: 599-610 (1993).
[51] Gruhn N.E., da Silva Filho D.A., Bill T.G., Malagoli M., Coropceanu V., Kahn A., Brédas J.-L., The Vibrational Reorganization Energy in Pentacene: Molecular Influences on Charge Transport, *J. Am. Chem. Soc.*, **124(27)**: 7918-7919 (2002).
[52] Bromley S.T., Mas-Torrent M., Hadley P., Rovira C., Importance of Intermolecular Interactions in Assessing Hopping Mobilities in Organic Field Effect Transistors: Pentacene Versus Dithiophene-Tetrathiafulvalene, *J. Am. Chem. Soc.*, **126(21)**: 6544-6545 (2004).
[53] Irfan A., Modeling of Efficient Charge Transfer Materials of 4,6-Di(Thiophen-2-Yl)Pyrimidine Derivatives: Quantum Chemical Investigations, *Comp. Mater. Sci.*, **81(0)**: 488-492 (2014).
[54] Irfan A., Cui R., Zhang J., Hao L., Push–Pull Effect on the Charge Transfer, and Tuning of Emitting Color for Disubstituted Derivatives of Mer-Alq3, *Chem. Phys.*, **364(1–3)**: 39-45 (2009).